

Inverse Halftoning Based on the Bayesian Theorem

Yun-Fu Liu, *Student Member, IEEE*, Jing-Ming Guo, *Senior Member, IEEE*, and Jiann-Der Lee, *Member, IEEE*

Abstract—This study proposes a method which can generate high quality inverse halftone images from halftone images. This method can be employed prior to any signal processing over a halftone image or the inverse halftoning used in JBIG2. The proposed method utilizes the least-mean-square (LMS) algorithm to establish a relationship between the current processing position and its corresponding neighboring positions in each type of halftone image, including direct binary search, error diffusion, dot diffusion, and ordered dithering. After which, a referenced region called a support region (SR) is used to extract features. The SR can be obtained by relabeling the LMS-trained filters with the order of importance. Moreover, the probability of black pixel occurrence is considered as a feature in this work. According to this feature, the probabilities of all possible grayscale values at the current processing position can be obtained by the Bayesian theorem. Consequently, the final output at this position is the grayscale value with the highest probability. Experimental results show that the proposed method offers better visual quality than that of Mese–Vaidyanathan’s and Chang *et al.*’s methods in terms of human-visual peak signal-to-noise ratio (HPSNR). In addition, the memory consumption is also superior to Mese–Vaidyanathan’s method.

Index Terms—Bayesian theorem, error diffusion, halftone image classification, halftoning, inverse halftoning.

I. INTRODUCTION

DIGITAL halftoning [1], [2] is a technique for converting continuous-tone images into limited-tone images. Halftone images (H) resemble an original grayscale images when viewed from a distance, due to the low-pass filtering nature of the human visual system (HVS). The technique is used widely in computer printouts, printed books, newspapers and magazines, as they are mostly constrained to black-and-white format (with and without ink). Another major application of digital halftoning is color quantization with a restricted color palette. Halftoning methods include ordered dithering (OD) [1], dot diffusion (DD) [3], [4], error diffusion (ED) [5]–[16] and an iteration-based halftoning: direct binary search (DBS) [17]–[22].

Inverse halftoning is a conjugate technique to halftoning, which restores an H with binary bit-depth to a continuous-tone image with multiple bit-depths. This technique can be employed for halftone image processing. For instance, inverse halftoning

can be used in image rotation, intensity changing, or image size adjustment. These signal processes significantly decrease image quality, since the processed results may become in continuous-tone fashion as opposed to the desired halftone binary format. Thus, an H is generally transformed to a grayscale image using inverse halftoning and then undergone those signal processing. The second round halftoning is applied to recover the halftone format after signal processing. In addition, inverse halftoning is also a part of the JBIG2 compression method. It is known that a binary image cannot achieve high compression ratio. Hence, inverse halftoning is employed in JBIG2 to obtain a grayscale image and then compressed for transmission. The decoder conducts the second round halftoning to recover the binary format for printing. In Chang-Yu’s study [23], the classification mechanism for different kinds of H takes priority over the algorithm of inverse halftoning so as to increase the resulting quality of inverse halftone images (IH). First, they tried transforming the H into their Fourier spectrums in order to separate different H . However, the complexity is inadmissible. Hence, the method was replaced by the cooperation between 1-D correlation and a three-layer backpropagation neural (BPN) network. Mese–Vaidyanathan’s inverse halftoning [24] is a look-up table (LUT) based method for all kinds of H . The resulting images have clear edges and this method is computationally efficient. In addition, the memory consumption is based upon the halftone value of possible combinations of all pixels in the referenced region. Consumption increases by 2^L , where L denotes the referenced number of pixels on H . Chang *et al.* [25] proposed a hybrid inverse halftoning technique. They employed the least-mean-square (LMS) to train masks to obtain the grayscale value when an empty cell is encountered. After which, the minimum mean square error (MMSE) was proposed for inverse halftoning, which also was a LUT-based method. This method offers excellent processing speed. In this work, the concept of Chang-Yu’s halftone image classification was adopted. Moreover, Bayesian theorem can provide a good classified result based upon the known information. As documented in [26], the Bayesian can achieve an optimal classified result when appropriate features are employed. This work adopts the probability of black pixel occurrence as the feature to cooperate with the Bayesian theorem. The experimental results prove that good reconstructed image quality can be achieved.

The rest of this study is organized as follows. Section II describes the proposed inverse halftoning method in detail. Section III presents the performance and experimental results, and conclusions are drawn in Section IV.

II. PROPOSED INVERSE HALFTONING BASED UPON THE BAYESIAN THEOREM

Fig. 1 shows the proposed inverse halftoning algorithm. The objective of this algorithm is to transform H into IH. First, the

Manuscript received December 29, 2009; revised April 12, 2010, June 29, 2010, August 17, 2010; accepted October 05, 2010. Date of publication October 18, 2010; date of current version March 18, 2011. The associate editor coordinating the review of this manuscript and approving it for publication was Mr. Vishal Monga.

Y.-F. Liu and J.-M. Guo are with the Department of Electrical Engineering, National Taiwan University of Science and Technology, Taipei 10607, Taiwan (e-mail: yunfuliu@gmail.com; jmguo@seed.net.tw).

J.-D. Lee is with the Department of Electrical Engineering, Chang Gung University, Taoyuan 33302, Taiwan (e-mail: jdlee@mail.cgu.edu.tw).

Digital Object Identifier 10.1109/TIP.2010.2087765

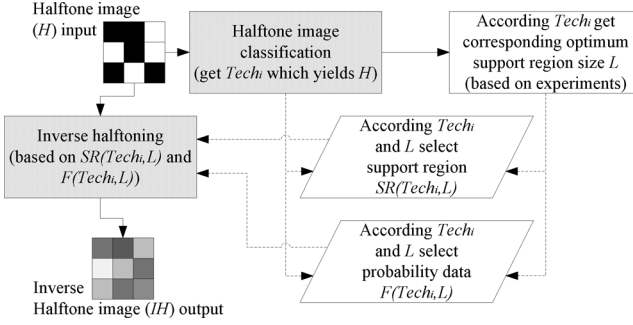


Fig. 1. Proposed inverse halftoning algorithm.

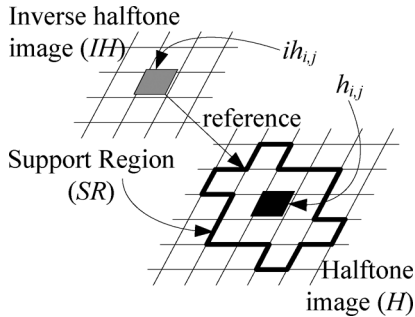


Fig. 2. Relationships among H, IH, and SR.

halftoning technique ($Tech_i$) which yields H should be determined prior to inverse halftoning, because different halftoning schemes have various characteristics. Thus, the H classification procedure is conducted in the first phase. Next, based upon the prior knowledge of $Tech_i$, the optimized support region (SR) size (L) can be determined to offer the best image quality for different kinds of H inputs. The parameter L is obtained from experiments which will be discussed in Section III. Two types of data are also involved in the proposed inverse halftoning, SR and probability data of feature (F), which is affected by $Tech_i$ and the corresponding L . The parameters SR and F are detailed in Sections II-A and II-B, respectively. As the parameters mentioned previously are determined, the proposed Bayesian-based inverse halftoning is employed to yield the corresponding inverse halftoning images. This process is explained in Section II-C.

A. SR

The transformation from H into grayscale images yields a damaged image, since the halftoning procedure is irreversible. In inverse halftoning, the H is the only information which can be referred to. To obtain a grayscale value from an IH $ih_{i,j} \in IH$, the information around position (i,j) is normally the best candidate. The neighboring region which provides such information is called the SR in this study. Fig. 2 shows the relationships among the H , IH , and SR. A question related to SR can be as follows: what kind of SR shape can effectively produce an accurate $ih_{i,j}$ for different types of halftoning? Apparently, each halftoning scheme should have an exclusive SR. Two parameters can determine a SR: 1) size and 2) referenced positions. Size implies the number of referenced pixels in an original H , and the referenced positions represent the shape of the SR. In

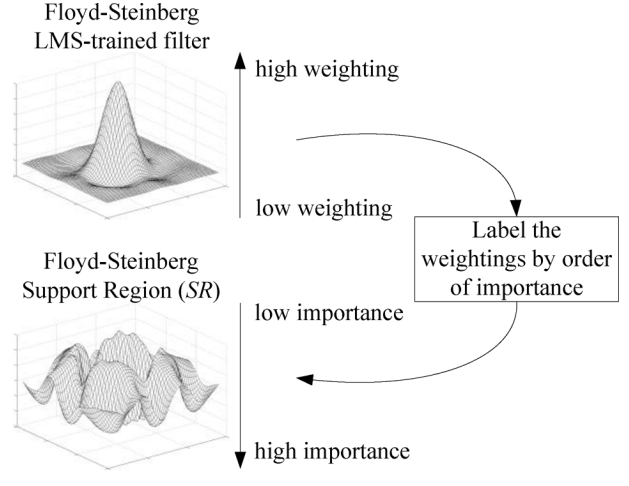


Fig. 3. LMS-trained SR.

this work, LMS is employed to determine the optimum referenced positions under a fixed SR size. The SR also represents the order of importance for yielding $ih_{i,j}$. In practice, we derive the order of importance by employing a training set of pairs of grayscale images and its corresponding halftone results. In this work, the iteration-based halftoning DBS, three kinds of error diffusion and DD, as well as two kinds of OD are adopted to produce the set (18 grayscale images + 18 corresponding $H \times 9$ halftoning methods). All the training image sets are from [27]. The LMS is employed to derive the order of importance of the SR as described in the following:

$$\hat{h}_{i,j} = \sum_{m,n \in SR} \sum_{k} w_{m,n}^k h_{i+m,j+n} \quad (1)$$

$$e_{i,j}^2 = (\text{ori}_{i,j} - \hat{h}_{i,j})^2 \quad (2)$$

$$\frac{\partial e_{i,j}^2}{\partial w_{m,n}} = -2e_{i,j} h_{i+m,j+n} \quad (3)$$

$$w_{m,n}^{k+1} = w_{m,n}^k + \begin{cases} \mu e_{i,j} h_{i+m,j+n}, & \text{if } \frac{\partial e_{i,j}^2}{\partial w_{m,n}} < 0 \\ -\mu e_{i,j} h_{i+m,j+n}, & \text{if } \frac{\partial e_{i,j}^2}{\partial w_{m,n}} > 0 \end{cases} \quad (4)$$

where the variables $\text{ori}_{i,j}$ and $h_{i,j}$ denote the pixel value in original grayscale image and the corresponding H at position (i,j) , respectively. The $w_{m,n}^k$ denotes the k th iteration weight at position (m,n) in the SR. The SR is of size 17×17 to fully represent 100% grayscale values, as discussed in the following. The variable μ denotes the adjusting parameter used to control the convergent speed of the LMS optimization procedure. In this work, the variable μ is set at 10^{-5} . According to our former experience, which is the largest variable that can guarantee convergent results, and any values smaller than this will lead to copious convergent time. The iteration is terminated when the square error $e_{i,j}^2$ does not change. Fig. 3 shows a sample of an LMS-trained filter (SR) from Floyd-Steinberg's error-diffused H . The trained filters of the previous nine halftoning schemes have three characteristics: 1) only the H obtained by error diffusion have a biased weight, because the error kernels only diffuse to nonprocessed pixel positions (causal operation); 2) the highest peak of importance around the center of each LMS-trained filter is directly proportional to the level of visual pleasure perceived by

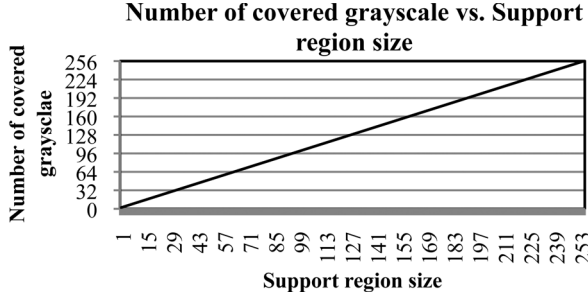


Fig. 4. Number of covered grayscales subject to SR size.

human eyes; 3) the diagonal has less sensitivity than vertical and horizontal directions, except for the case of DBS since this type of halftoning has no apparent direction. Finally, the SR(Tech_i) can be obtained by relabeling the weight by order of importance, corresponding to the LMS-trained filter. According to this procedure, different halftoning SRs SR(Tech_i) can be obtained, which are suited for the corresponding Tech_i . When a SR with different support size L is needed, we can keep discarding the positions with lowest importance from SR until the size is met.

Basically, the $ih_{i,j}$ is affected by the $h_{i+m,j+n}$, where $m, n \in \text{SR}$, and halftone values in the SR with higher importance have more influences in $ih_{i,j}$. On the other hand, the $ih_{i,j}$ is the joint result from all halftone values in SR, and the accurate value is affected by the proportion of the number of black pixels and white pixels in the SR. For example, if the number of black pixels is greater than white pixels, then $ih_{i,j}$ tends to be 0. Conversely, the $ih_{i,j}$ tends to be 255. According to this phenomenon, the relationship between the represented grayscale values (g_R) and the corresponding black and white pixel numbers can be expressed by the following:

$$g_R = \text{round} \left(\frac{N_w \times 255}{N_w + N_b} \right) \quad (5)$$

where variables N_w and N_b denote the number of white and black pixels required to represent the grayscale value g_R . The function $\text{round}(\cdot)$ represents rounding off to the nearest integer. The required total number of pixels which is obtained from $N_w + N_b$ represents the required size of the SR. According to the previous equation, the relationship between SR size and the corresponding number of g_R can be obtained. Fig. 4 shows the linear relation between SR size and the number of covered grayscale. It can be seen that when SR size is smaller than 255, it cannot fully represent all the grayscales. Also, the size of the SR is expected to be in odd number. Thus, the SR of size 17×17 is adopted for LMS training procedure to represent all grayscale values. Based upon this observation, the g_R can be employed to reduce the memory consumption and increase accuracy in predicting the original grayscale value of the currently processed pixel. This process is discussed in the next subsection.

B. Feature

Different densities of black pixels in H can render different grayscales, and different halftone patterns have different dot distributed textures. According to this concept, a feature (F) is employed in this study to accurately predict $ih_{i,j}$ which is the probability of black pixel occurrence at each position in the SR. The

adopted feature gears with the previous two characteristics of an H .

To obtain the feature (F), 153 natural training images of size 512×512 were employed. This set is different from the set used for the training SR in Section II-A, but this set is also constructed from [27]'s database. First, select a halftoning technique Tech_i and the corresponding $\text{SR}(L, \text{Tech}_i)$ with limited SR size L . Mese–Vaidyanathan's inverse halftoning [24] checks the combinations of black and white pixels in the SR with limited L to find the grayscale value of the current processing pixel. The memory consumption of this method increases by 2^L , which means this method requires a lot of memory. To solve this problem, it is replaced by the probability of black pixel occurrence at each position in the SR. The memory consumption is, thus, reduced to $N_{g_R} \times L$, where variable N_{g_R} denotes the number of g_R in limited L . The probability is described as

$$p(h_{i+m,j+n} = 0 | \text{ori}_{i,j} \in g_R) = \frac{\text{Num}(h_{i+m,j+n} = 0 | \text{ori}_{i,j} \in g_R)}{\text{Num}(\text{ori}_{i,j} \in g_R)} \quad (6)$$

where position $(m, n) \in \text{SR}(L, \text{Tech}_i)$, and function $\text{Num}(\cdot)$ denotes the calculation of counts occurred for a given event. In the explanation of Section II-A, N_{g_R} cannot be 256 except for the cases when L is greater or equal to 255, and under common condition the L is further lower than 255, this makes the N_{g_R} is also lower than 256 with the relationship of Fig. 4. According to this, in the procedure of statistical probability construction as (6), the $\text{ori}_{i,j}$ only needs to take g_R into consideration since others cannot be represented under this limitation on SR size L . This strategy can significantly reduce the memory consumption.

C. Inverse Halftoning Technique Based Upon the Bayesian Theorem

The performance of inverse halftoning techniques are determined by the degree of similarity between original image (Ori) and IH obtained with limited information. The Bayesian theorem is a fundamental probabilistic approach to the problem of classification, which can obtain an optimum decision based upon all known probabilistic features. Based upon these features, the probability of the various grayscale values at the position currently being processed can be determined. The conditional probability is described as follows:

$$p(g_q | h_0, h_1, \dots, h_{L-1}) = \frac{p(g_q \cap h_0, h_1, \dots, h_{L-1})}{p(h_0, h_1, \dots, h_{L-1})} \quad (7)$$

where variable g_q denotes grayscale value q , where $q \in g_R$, and variable h_k denotes the halftone value of the neighbor position with k th order of importance in $\text{SR}(L, \text{Tech}_i)$. Focusing on the numerator, the previous equation can be rewritten as follows:

$$p(g_q | h_0, h_1, \dots, h_{L-1}) = \frac{p(g_q)p(h_0, h_1, \dots, h_{L-1}|g_q)}{p(h_0, h_1, \dots, h_{L-1})} \quad (8)$$

where $p(g_q)$ is called priori probability, $p(h_0, h_1, \dots, h_{L-1}|g_q)$ is called the likelihood of g_q with respect to these features

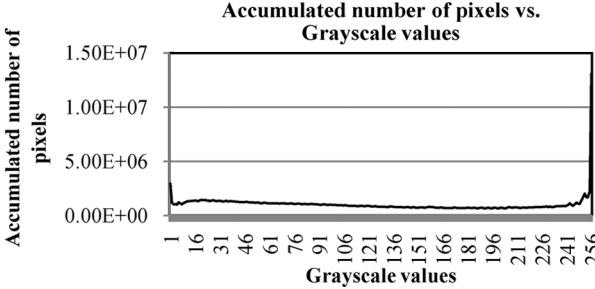


Fig. 5. Practical grayscale distribution with 1000 test images [27].

h_0, h_1, \dots, h_{L-1} , and $p(h_0, h_1, \dots, h_{L-1})$ is called the evidence. The memory consumption of the numerator is $N_{g_R} \times 2^L$, where the $p(g_q)$ is assumed as an uniform distribution ($1/N_{g_R}$) in this study, and the other parts are used for searching the mapping probability of $p(h_0, h_1, \dots, h_{L-1}|g_q)$. Normally, the distribution $p(g_q)$ for a well exposed image should be Gaussian, However, in our experience, not all of the natural images are well exposed candidates. Herein, 1000 common natural images [27], including the 153 training and the 202 testing images used in this work, are employed for generating the corresponding distribution. As it can be seen from Fig. 5, the result is close to the uniform distribution as we suggested. Thus, without losing generality by simply using the Gaussian distribution for ideal exposed images, the uniform distribution is employed to better characterize the property of the most digital images. To simplify the implementation, the previous equation is rewritten as follows to let all features be independent. The independent assumption is from the Naïve Bayes classifier, which has been proven that it still can maintain excellent performance from Zhang's research [26]

$$p(g_q|h_0, h_1, \dots, h_{L-1}) = \frac{p(g_q) \prod_{k=0}^{L-1} p(h_k|g_q)}{p(h_0, h_1, \dots, h_{L-1})}. \quad (9)$$

In this way, the memory consumption is reduced to $N_{g_R} \times L$. As for the evidence, it is probably changed when H is different from the first trained H. For this reason, the evidence is redescribed by the Bayesian theorem as follows:

$$\begin{aligned} p(g_q|h_0, h_1, \dots, h_{L-1}) \\ = \frac{p(g_q) \prod_{k=0}^{L-1} p(h_k|g_q)}{\sum_{r \in g_R} [p(g_r) \prod_{k=0}^{L-1} p(h_k|g_r)]}. \end{aligned} \quad (10)$$

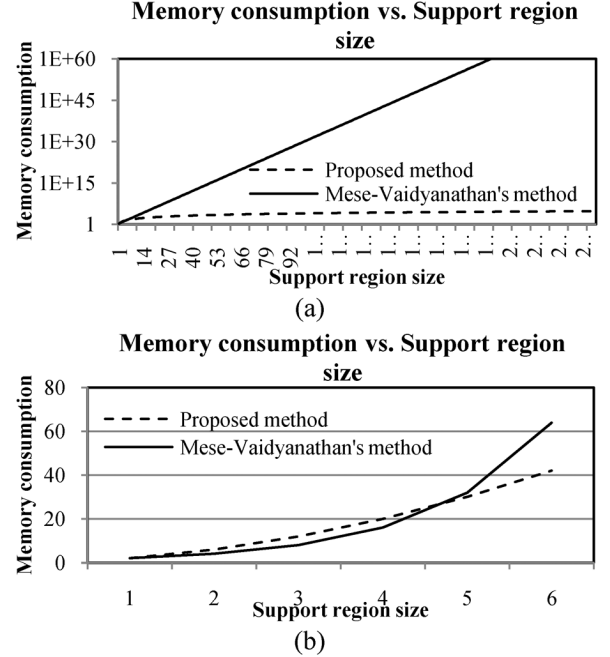


Fig. 6. Comparison of memory consumption between the proposed method and Mese-Vaidyanathan's method [24]. (a) Vertical axis is compressed by $\log(\cdot)$. (b) Reduced the range of horizontal axis from 1 to 6.

Besides, the probabilities of all g_R are obtained. Finally, the $ih_{i,j}$ can be obtained by the following:

$$ih_{i,j} = \arg \max_{q \in g_R} [p(g_q|h_0, h_1, \dots, h_{L-1})]. \quad (11)$$

According this method, the IH can be obtained.

III. EXPERIMENTAL RESULTS

In this section, we apply the proposed Bayesian-based inverse halftoning for quantitative evaluation. A comparison of the memory consumption of the proposed method with that of Mese-Vaidyanathan's inverse halftoning [24] is shown in Fig. 6. This figure represents the amount of required memory at the size L of different SRs. The vertical axis of Fig. 6(a) is compressed by log function since we can observe that the memory consumption of Mese-Vaidyanathan's method is increased by power law. The range of different SR sizes from 1 to 6 is shown in Fig. 6(b).

$$HPSNR = 10 \log_{10} \left(\frac{P \times Q \times 255^2}{\sum_{i=1}^P \sum_{j=1}^Q [\sum_{m,n \in GF} coe_{m,n} (\text{ori}_{i+m,j+n} - ih_{i+m,j+n})]^2} \right) \quad (12)$$

$$coe_{m,n} = \frac{1}{2\pi\sigma_m\sigma_n\sqrt{1-\rho^2}} \times e^{-\frac{1}{2(1-\rho^2)} \left[\frac{(m-\mu_m)^2}{\sigma_m^2} - 2\rho \left(\frac{m-\mu_m}{\sigma_m} \right) \left(\frac{n-\mu_n}{\sigma_n} \right) + \frac{(n-\mu_n)^2}{\sigma_n^2} \right]} \quad (13)$$

	Mese-Vaidyanathan's method [24]	Proposed method		
Original grayscale image			M08 [4]	 HPSNR=34.68 dB
DBS [20]	 HPSNR=38.83 dB	 HPSNR=38.95 dB	M16 [4]	 HPSNR=36.88 dB
Flo [5]	 HPSNR=39.71 dB	 HPSNR=41.83 dB	Clu [1]	 HPSNR=28.05 dB
Jar [6]	 HPSNR=36.80 dB	 HPSNR=40.28 dB	Dis [1]	 HPSNR=33.60 dB
Stu [7]	 HPSNR=37.48 dB	 HPSNR=40.93 dB		 HPSNR=34.09 dB
Knu [3]	 HPSNR=34.37 dB	 HPSNR=35.36 dB		

Fig. 7. Inverse halftoning results with SR size 16, two methods are included, Mese–Vaidyanathan's [24] and proposed methods (all printed at 450 dpi).

The memory consumption of Mese–Vaidyanathan's method is superior to the proposed method that ranges from 1 to 4. However, it cannot provide better IH quality for different halftoning techniques with SR size as small as 4.

For image quality assessment, The traditional PSNR indeed is not suited for characterizing the response of human vision, since the distortions (MSE) between the original image and a reconstructed image is calculated pixel-wised. Normally, when we perceive an image, the information of the neighboring pixels is included. Thus, we modify the definition of PSNR to human-visual peak signal-to-noise ratio (HPSNR) to better characterize the response of the human visual system. Suppose the image is of size $P \times Q$, and the quality is defined as shown in (12)

and (13) at the bottom of the previous page, where the variable $coe_{m,n}$ is employed for representing the low-pass characteristic of HVS. In this study, $coe_{m,n}$ is obtained by the following 2-D Gaussian filter (GF) of size 7×7 . Notably, the parameter can be modified, but the order of the performances among the proposed method and former approaches are still consistent according to our experiments. where the variable μ denotes the mean, the variable ρ denotes the correlation coefficient, and the variable σ denotes standard deviation. In this work, $\sigma = 1.3$ and $\rho = 0$. The reason for choosing the parameter configuration is identical to that of GF size.

Table I shows the comparison of the image quality of two kinds of inverse halftoning, which include Chang *et al.*'s method

TABLE I
COMPARISON OF IMAGE QUALITY WITH DIFFERENT INVERSE HALFTONING AND HALFTONING

Inverse halftoning	Halftoning	Clu [1]	Dis [1]	Jar [6]
Chang et al.'s method [25] (SR=21)	Lena	26.96 dB	28.20 dB	31.64 dB
	Peppers	26.89 dB	28.26 dB	31.23 dB
	Lake	24.46 dB	25.96 dB	29.31 dB
	Average	26.10 dB	27.47 dB	30.73 dB
Mese-Vaidyanathan's method [24]	Lena	27.91 dB	33.31 dB	37.03 dB
	Peppers	27.46 dB	33.15 dB	35.99 dB
	Lake	27.49 dB	31.69 dB	33.91 dB
	Average	27.62 dB	32.72 dB	35.64 dB

[25] and Mese–Vaidyanathan's method [24]. Herein, clustered-dot (abbr.: Clu) and dispersed-dot dithering (abbr.: Dis) [1], and Jarvis *et al.*'s error diffusion (abbr.: Jar) [6] H are employed for testing. Results indicate that Mese–Vaidyanathan's method obtains the better image quality in all cases. According to these results, we focus on the comparison of Mese–Vaidyanathan's method and the proposed method. First, the size of SR is fixed at 16 to provide a fair comparison condition, since in [24], Mese and Vaidyanathan employed SR of size 16 for inverse halftoning. The corresponding results are shown in Fig. 7. Herein, six more halftoning techniques are employed for testing, which include Agar–Allebach's DBS [20], Floyd–Steinberg's error diffusion (abbr.: Flo) [5], Stucki's error diffusion (abbr.: Stu) [7], Knuth's DD (abbr.: Knu) [3], and Mese–Vaidyanathan's DD [4] with 8×8 class matrix size (abbr.: M08) and 16×16 (abbr.: M16). Among these results, Mese–Vaidyanathan's method expresses the high frequency parts well, such as the left zipper on the clothing of the girl. However, the expression of the ramp low frequency parts, such as the top-right corner of this image, is inferior to the proposed method, except for the H obtained by dispersed-dot dithering. This is because dispersed-dot dithering itself has false contour in the corresponding regions. One interesting phenomenon observed in Fig. 7 is that Mese–Vaidyanathan's method yields sharper results than the proposed method with those error diffused images and, thus, it infers that the proposed method can provide the additional feature of desharpening. The reason is straightforward: Despite many possible textures, including sharpening, exist in various halftone patterns from various halftoning techniques, the proposed Bayes-based inverse halftoning always learns from the original images during the training phase. Thus, it always can generate those desharpended inverse results from sharpened halftone patterns obtained by the error-diffusion-based halftoning schemes.

The proposed method can reduce the memory consumption, and the memory usage is very stable at it can be seen in Fig. 6(a). Thus, even the SR sizes for each halftoning technique is optimized by using different values, the memory consumption still can be maintained rather stable. Conversely, in Mese–Vaidyanathan's method if the SR size is changed, the memory consumption will probably go extremely high. Consequently, in this study an experiment is conducted using nine various halftoning techniques for establishing the relationship between average HPSNR and the corresponding SR sizes, as shown in Fig. 8. The average HPSNR is obtained from 202 test images of size 512×512 , which are different from the

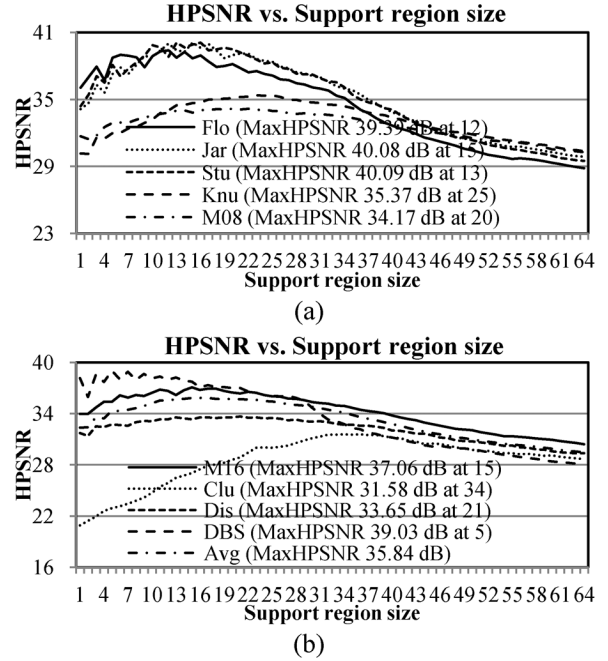


Fig. 8. Average HPSNR of various types of halftoning techniques when different SR sizes from 1 to 64 are applied.

set used for training feature or SR. Moreover, the SR size is constrained from 1 to 64, since the bigger SR sizes cannot yield a better performance. According to these results, each halftoning technique indeed has a specific optimum SR size as observed in the following. The halftoning techniques which can yield better halftone quality are with smaller optimum SR sizes, and vice versa. Fig. 9 shows the results when the optimum SR sizes are employed for the corresponding H. Apparently, all the results obtained with the proposed method are with better image quality. Yet, an interesting observation that the inverse result from DBS is inferior to that of the three error diffusion results. Since the proposed Bayesian-based inverse halftoning technique utilizes the training image set for prediction. The Error diffusion schemes we employed in this work, such as Floyd–Steinberg's, Jarvis *et al.*'s, and Stucki's, all use the error kernel and similar processing path, and which make the possible halftone patterns in a specific SR simply occupy a small set of the maximum possibility (2^N , where N denotes the bit-stream length). In contrast, the DBS utilizes toggle and swap two operations to iteratively optimize the halftone pattern, which makes the dot distribution difficult to predict, and the possible halftone patterns in a specific SR close to the maximum possibility. Thus, due to the possible number of pattern combinations in error diffusion is fewer than that of the DBS, the predicting accuracy of error diffusion is also superior to that of the DBS. As a result, the PSNR of inverse halftone from DBS cannot outperform error diffusion. Fig. 10 shows the average HPSNRs using the previous 202 test images, which includes the comparisons between Mese–Vaidyanathan's method and the proposed method with SR of size 16, and the proposed method with optimum SR size. All the results demonstrate that the proposed method is fully superior to that of Mese–Vaidyanathan's method in all halftoning cases.

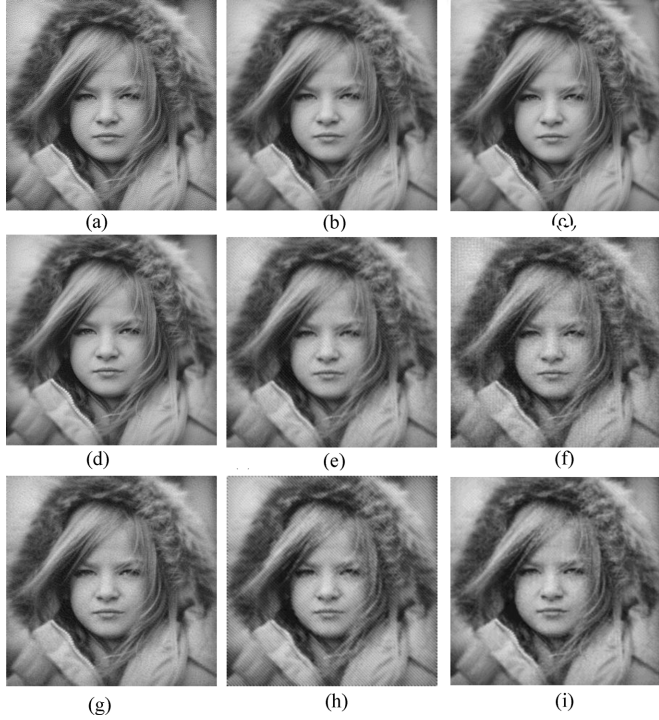


Fig. 9. IH using the proposed method with the corresponding optimum SR size. (a) Agar-Allebach's DBS [20] with SR size of 5. (b) Floyd-Steinberg's error diffusion [5] with SR size of 12. (c) Jarvis *et al.*'s error diffusion [6] with SR size of 15. (d) Stucki's error diffusion [7] with SR size of 13. (e) Knuth's DD [3] with SR size of 25. (f) Mese-Vaidyanathan's DD [4] with class matrix of size 8×8 and SR size of 20, and (g) with class matrix of size 16×16 and SR size of 15. (h) Ulichney's [1] clustered-dot dithering with SR size of 34, and (i) dispersed-dot dithering with SR size of 21. (all printed at 350 dpi) (a) HPSNR = 38.34 dB, (b) HPSNR = 41.83 dB, (c) HPSNR = 41.62 dB, (d) HPSNR = 41.76 dB, (e) HPSNR = 36.33 dB, (f) HPSNR = 34.30 dB, (g) HPSNR = 36.86 dB, (h) HPSNR = 31.91 dB, and (i) HPSNR = 34.48 dB.

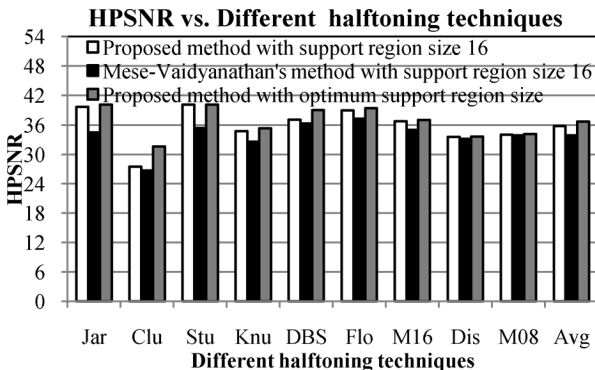


Fig. 10. Image quality comparisons between the proposed method and Mese-Vaidyanathan's method under various halftone schemes with average HPSNR from 202 natural images.

IV. CONCLUSION

In this work, a Bayesian-based inverse halftoning for nine different types of halftoning is proposed. This method employs LMS to determine the importance of the neighboring positions in the SR. Moreover, the probability of the black pixel occurrence at each position in the SR is employed as a feature to precisely predict the grayscale values of an IH. In experimental results, the image quality obtained by the proposed method

is superior to that of Chang *et al.*'s inverse halftoning. When the original H are produced by those schemes which can yield good image quality, such as error diffusion, DBS, and DD with Mese-Vaidyanathan's 16×16 class matrix, the expression on the ramp low frequency part of Mese-Vaidyanathan's inverse halftone results is inferior to the proposed method. Moreover, in terms of memory consumption, although the proposed method is inferior to Mese-Vaidyanathan's inverse halftoning when the SR is of sizes from 1 to 4, yet the optimum SR sizes of all halftoning techniques in the experimental results are always bigger than 4. Thus, the memory consumption is still an advantage of the proposed work.

In this work, the type, e.g., error diffusion and OD, of a given H is assumed as prior knowledge. Since H classification plays an important role before the proposed inverse halftoning can be applied, we will look for more effective ways to precisely classify different halftone patterns. Also, this work employs a feature to predict an IH. In fact, the mean of all the halftone values in SR was also taken into account. Yet, the corresponding results yielded similar quality as the results when simply one feature is employed. In addition, more memory is required for the additional feature. Thus, the probability of black pixel occurrence is employed as the single feature in this work. More effective features are left for future exploration to further improve image quality.

Although the proposed scheme can provide superior image quality for those natural images in terms of HPSNR, the proposed method seems render inferior quality to that of Mese-Vaidyanathan's method in those "special cases (details)." We admit which can be a weakness of the proposed scheme. Yet, when it comes to a normal natural image, we found that most of the components in an image are rather smooth with low frequency textures. Thus, the proposed method mostly can generate a good image quality with natural images in terms of HPSNR, and consequently it can be considered as a good candidate for most applications which requires inverse halftoning. Future possible working directions can be put to develop a hybrid method, such as combining Mese-Vaidyanathan's work and the proposed method, to fully take care of all the possible components, smooth or detail, in an image.

REFERENCES

- [1] R. Ulichney, *Digital Halftoning*. Cambridge, MA: MIT Press, 1987.
- [2] D. L. Lau and G. R. Arce, *Modern Digital Halftoning*. New York: Marcel Dekker, 2001.
- [3] D. E. Knuth, "Digital halftones by dot diffusion," *ACM Trans. Graph.*, vol. 6, no. 4, Oct. 1987.
- [4] M. Mese and P. P. Vaidyanathan, "Optimized halftoning using dot diffusion and methods for inverse halftoning," *IEEE Trans. Image Process.*, vol. 9, no. 4, pp. 691–709, Apr. 2000.
- [5] R. W. Floyd and L. Steinberg, "An adaptive algorithm for spatial gray scale," in *Proc. SID '75 Digest. Soc. Inf. Display*, 1975, pp. 36–37.
- [6] J. F. Jarvis, C. N. Judice, and W. H. Ninke, "A survey of techniques for the display of continuous-tone pictures on bilevel displays," *Comput. Graph. Image Process.*, vol. 5, no. 1, pp. 13–40, 1976.
- [7] P. Stucki, "MECCA-A multiple-error correcting computation algorithm for bilevel image hardcopy reproduction," IBM Res. Lab., Zurich, Switzerland, Res. Rep. RZ1060, 1981.
- [8] V. Ostromoukhov, "A simple and efficient error-diffusion algorithm," *Comput. Graph.*, pp. 567–572, 2001.
- [9] L. Velho and J. M. Gomes, "Digital halftoning with space filling curves," *Comput. Graph.*, vol. 25, no. 4, pp. 81–90, Jul. 1991.

- [10] K. T. Knox, "Introduction to digital halftones," in *Proc. Recent Progress in Digital Halftoning*, R. Eschbach, Ed., 1994, pp. 30–33.
- [11] J. N. Shiau and Z. Fan, "Set of easily implementable coefficients in error diffusion with reduced worm artifacts," in *Proc. SPIE Color Imag.*, 1996, vol. 2658, pp. 222–225.
- [12] R. Eschbach, "Reduction of artifacts in error diffusion by mean of input-dependent weights," *J. Electron. Imag.*, vol. 2, no. 4, pp. 352–358, 1993.
- [13] P. Li and J. P. Allebach, "Tone-dependent error diffusion," *IEEE Trans. Image Process.*, vol. 13, no. 2, pp. 201–215, Feb. 2004.
- [14] P. Li and J. P. Allebach, "Block interlaced pinwheel error diffusion," *J. Electron. Imag.*, vol. 14, no. 2, pp. 1–13, Apr.–Jun. 2005.
- [15] T. C. Chang and J. P. Allebach, "Memory efficient error diffusion," *IEEE Trans. Image Process.*, vol. 12, no. 11, pp. 1352–1366, Nov. 2003.
- [16] B. L. Evans, V. Monga, and N. Damera-Venkata, "Variations on error diffusion: Retrospectives and future trends," in *Proc. SPIE Color Imag.*, Jan. 2003, vol. 5008, pp. 371–389.
- [17] Q. Lin and J. P. Allebach, "Color FM screen design using DBS algorithm," in *Proc. SPIE Color Imag.*, 1998, vol. 3300, pp. 353–361.
- [18] A. U. Agar and J. P. Allebach, "Model-based color halftoning using direct binary search," *IEEE Trans. Image Process.*, vol. 14, no. 12, pp. 1945–1959, Dec. 2005.
- [19] F. A. Baqai and J. P. Allebach, "Halftoning via direct binary search using analytical and stochastic printer models," *IEEE Trans. Image Process.*, vol. 12, no. 1, pp. 1–15, Jan. 2003.
- [20] M. Analoui and J. P. Allebach, "Model based halftoning using direct binary search," in *Proc. SPIE, Human Vis., Visual Proc., Dig. Display III*, Feb. 1992, vol. 1666, pp. 96–108.
- [21] D. J. Lieberman and J. P. Allebach, "Model based direct binary search halftone optimization with a dual interpretation," in *Proc. IEEE Int. Conf. Image Process.*, Oct. 1998, vol. 2, pp. 44–48.
- [22] J. P. Allebach and Q. Lin, "FM screen design using DBS algorithm," in *Proc. IEEE Int. Conf. Image Process.*, Sep. 1996, vol. 1, pp. 549–552.
- [23] P.-C. Chang and C.-S. Yu, "Neural net classification and LMS reconstruction to halftone images," in *Proc. SPIE Vis. Commun. Image Process.*, Jan. 1998, vol. 3309, pp. 592–602.
- [24] M. Mese and P. P. Vaidyanathan, "Look-up table (LUT) method for inverse halftoning," *IEEE Trans. Image Process.*, vol. 10, no. 10, pp. 1566–1578, Oct. 2001.
- [25] P.-C. Chang, C.-S. Yu, and T.-H. Lee, "Hybrid LMS-MMSE inverse halftoning technique," *IEEE Trans. Image Process.*, vol. 10, no. 1, pp. 95–103, Jan. 2001.
- [26] H. Zhang, "The optimality of naïve Bayes," in *Proc. 7th Int. Florida Artif. Intell. Res. Soc. Conf.*, 2004, pp. 562–567.
- [27] [Online]. Available: <http://msp.ee.ntust.edu.tw/public%20file/ImageSet.rar>



Yun-Fu Liu (S'09) was born in Hualien, Taiwan on October 30, 1984. He received the M.S.E.E. degree from department of Electrical Engineering, Chang Gung University, Taoyuan, Taiwan, in 2009, and is currently pursuing the doctoral degree in the Department of Electronic Engineering, National Taiwan University of Science and Technology, Taipei, Taiwan.

His research interests include digital halftoning, digital watermarking, pattern recognition, and intelligent surveillance system.

Mr. Liu is a student member of the IEEE Signal Processing Society. He received the Special Jury Award from Chimei Innolux Corporation in 2009, and the third Master's Thesis Award from Fuzzy Society, R.O.C. in 2009.



Jing-Ming Guo (M'06-SM'10) was born in Kaohsiung, Taiwan, on November 19, 1972. He received the B.S.E.E. and M.S.E.E. degrees from National Central University, Taoyuan, Taiwan, in 1995 and 1997, respectively, and the Ph.D. degree from the Institute of Communication Engineering, National Taiwan University, Taipei, Taiwan, in 2004.

From 1998 to 1999, he was an Information Technique Officer with the Chinese Army. From 2003 to 2004, he was granted the National Science Council scholarship for advanced research from the

Department of Electrical and Computer Engineering, University of California, Santa Barbara. He is currently an Associate Professor with the Department of Electrical Engineering, National Taiwan University of Science and Technology, Taipei. His research interests include multimedia signal processing, multimedia security, digital halftoning, and digital watermarking.

Dr. Guo is a senior member of the IEEE Signal Processing Society. He received the Excellence Teaching Award in 2009, the Research Excellence Award in 2008, the Acer Dragon Thesis Award in 2005, the Outstanding Paper Awards from IPPR, Computer Vision and Graphic Image Processing in 2005 and 2006, and the Outstanding Faculty Award in 2002 and 2003.



Jiann-Der Lee (M'98) was born in Tainan, Taiwan, in 1961. He received the B.S., M.S., and Ph.D. degrees from the Department of Electrical Engineering, National Cheng Kung University, Taiwan, in 1984, 1988, and 1992, respectively.

He is currently a Full Professor with the department of Electrical Engineering, Chang Gung University, Tao-Yuan. His current research interests include image processing, pattern recognition, computer vision, consumer electronics and VLSI CAD design.

Dr. Lee is a member of IEEE and IAPR, and is listed in the Who's Who in the World, Who's Who in Finance and Industry. He received a number of investigator awards (e.g. from National Science Council, Taiwan, and Acer Foundations, Taiwan), the Excellent Teaching Award, 2002, and the Excellent Research Award, 2003, from the Chang Gung University.